

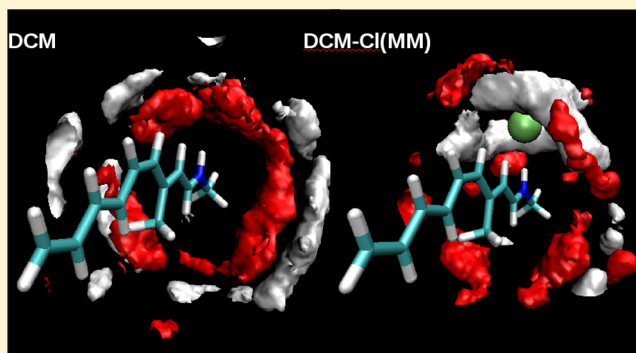
# Simultaneous Solvent and Counterion Effects on the Absorption Properties of a Model of the Rhodopsin Chromophore

Aurora Muñoz-Losa,\* Ignacio Fdez. Galván, Manuel A. Aguilar, and M. Elena Martín

Química Física, Universidad de Extremadura, Avda. de Elvas s/n, Badajoz, 06071, Spain

## Supporting Information

**ABSTRACT:** The ASEP/MD (averaged solvent electrostatic potential from molecular dynamics) method was employed in studying the environment effects (solvent and counterion) on the absorption spectrum of a model of the 11-*cis*-retinal protonated Schiff base. Experimental studies of the absorption spectra of the rhodopsin chromophore show anomalously large solvent shifts in apolar solvents. In order to clarify their origin, we study the role of the counterion and of the solute–solvent interactions. We compare the absorption spectra in the gas phase, cyclohexane, dichloromethane, and methanol. The counterion effect was described from both a classical and quantum point of view. In the latter case, the contribution of the chromophore–counterion charge transfer to the solvent shift could be analyzed. To the best of our knowledge, this is the first time that counterion and solvent effects on the absorption properties of the 11-*cis*-retinal chromophore have been simultaneously examined. We conclude that the counterion–solute ionic pair in the gas phase is not a good model to represent the solvent shift in nonpolar solvents, as it does not account for the effect that the thermal agitation of the solvent has on the geometry of the ionic pair. In contrast to nonpolar solvents, the experimental solvent shift values in methanol can be exclusively explained by the polarity of the medium. In dichloromethane, the presence of the counterion does not modify the solvent shift of the first absorption band, but it affects the position of the second excited state. In the three solvents considered, the first two excited states become almost degenerate.



## 1. INTRODUCTION

Rhodopsin has been largely studied in past decades due to its importance in the human vision process. Upon the absorption of a photon, its chromophore, the protonated Schiff base of the 11-*cis*-retinal molecule (PSB11), can undergo a *cis*–*trans* photoisomerization whose kinetics are modulated by the surrounding environment. Thus, inside the protein the isomerization takes place in about 200–500 fs,<sup>1,2</sup> while in a methanol solution, the process is slowed down to 10 ps probably because the chromophore twist implies a large solvent reorganization.<sup>3</sup> Experimental and theoretical studies have tried to analyze in depth the effect of the environment on the optical properties of this visual pigment. For instance, whereas in a vacuum<sup>4,5</sup> and in the protein<sup>6–8</sup> the absorption spectrum shows two bands that can be assigned to the first two electronic transitions, in solution<sup>9–11</sup> only a single wide band is found, which includes both electronic transitions. With respect to the de-excitation process, the most probable path implies an internal conversion that leads to the photoisomerization product; however, in solution, fluorescence is observed, a process that, despite its low quantum yield,<sup>9</sup> competes with the photoisomerization.

Experimental and theoretical studies have evidenced that the surrounding environment modifies to a great extent the photochemical and photophysical behavior of the PSB11

chromophore.<sup>12–22</sup> In the current work, we have focused on the study of the solvent and counterion effects on the electron absorption spectra of a model of the retinal chromophore in solution (M2 in Figure 1). From a theoretical point of view, the difficulties in the calculations of electron absorption spectra in solution are mainly due to the great number of solvent molecules involved, the manifold of configurations thermally accessible, and the interplay between solute and solvent dynamics, among others. In previous studies,<sup>11,12</sup> a complete analysis of the absorption and emission properties in methanol solution of a simplified five-bond model (M1, see Figure 1) was done using the ASEP/MD (average solvent electrostatic potential from molecular dynamics data) method.<sup>23</sup> Our results explained the PSB11 behavior in polar solvents such as the band shift in the absorption spectrum with respect to the gas-phase one, the existence of different radiative pathways from different S<sub>1</sub> minima, or the importance of nonradiative de-excitation pathways.

An intriguing fact regarding the absorption spectrum of PSB11 is that it displays anomalously high blue solvent shifts in nonpolar solvents.<sup>9</sup> Thus, it is found experimentally that the solvent shift suffered by the absorption band in a nonpolar

Received: December 12, 2012

Published: February 15, 2013

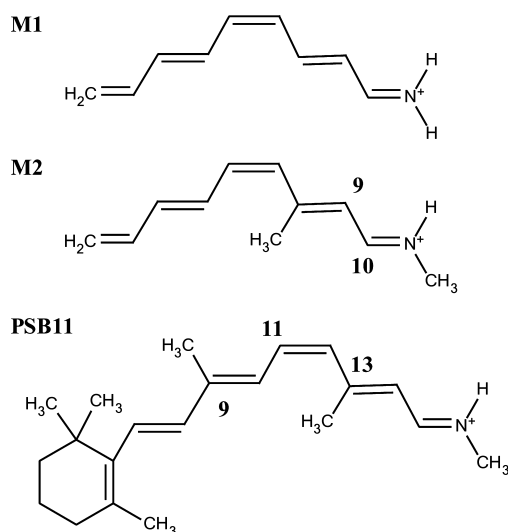


**Figure 1.** 11-*cis*-Retinal protonated Schiff base and some simplified models thereof.

solvent such as cyclohexane is quite similar to that of much more polar ones such as methanol or acetonitrile. Given that PSB11 is a charged molecule, it has been proposed that the counterion employed in these experiments plays an important role in its solvation, and hence it can modify the transition energies of the chromophore. A support to this hypothesis comes from theoretical calculations that have evidenced that the consideration of a chloride counterion in the gas phase causes a blue shift of the absorption band. So, Cembran et al.<sup>24</sup> found that when the chloride–nitrogen distance is 5.25 Å, the transition energy shift is equivalent to that measured in methanol. The environment also changes the emission band positions; in this sense, Zgrablić et al.<sup>9</sup> have shown experimentally that the emission values are strongly affected by the solvent polarity.

In the current study, the absorption spectra of two models of PSB11 in methanol were studied: the aforementioned M1, which is a five-double-bond model where all the methyl groups of the chromophore have been replaced by hydrogen atoms and where the  $\beta$ -iononic ring has been removed, and the M2 model, which differs from M1 in that it includes one methyl group linked to the nitrogen plus an additional methyl group in the 8 position (see Figure 1). In order to try to understand the origin of the abnormally high solvent shift in nonpolar solvents, the absorption spectrum of the more complete M2 model was analyzed in cyclohexane (cHex) and compared to that obtained in dichloromethane (DCM) and methanol (MeOH). Next, the effect of the counterion was analyzed. We perform two types of calculations depending on the description of the counterion during the QM/MM calculations: In the first set of calculations, the counterion and the solvent are both classically described during the MM simulations. In a second set, the counterion is included with the solute in the quantum part, and only the solvent is classically described. In this last case, the influence of the charge transfer from the counterion to the chromophore can be analyzed. For this task, an extended version of the ASEP/MD method was employed. To the best of our knowledge, this is the first time that counterion and solvent effects on the absorption properties of the PSB11 chromophore have been simultaneously studied.

## 2. METHOD AND DETAILS

Solvent effects on the ground and first two excited states of PSB11 and of two molecules that are frequently used as models of PSB11 (Figure 1) were studied with the ASEP/MD method. ASEP/MD is a QM/MM effective Hamiltonian method that makes use of the mean field approximation.<sup>23</sup> A scheme of ASEP/MD is presented in Figure S.1 in the Supporting Information. The method combines quantum mechanics (QM) and molecular dynamics (MD) techniques, with the particularity that QM and MD calculations are sequential and not simultaneous. During the MD simulations, the intramolecular geometry and charge distribution of the solute are considered fixed, but they are updated during the quantum calculation. The average electrostatic potential generated by the solvent on the solute is obtained from the MD data. This solvent potential is introduced as a perturbation into the solute's quantum mechanical Hamiltonian, and by solving the associated Schrödinger equation, a new charge distribution for the solute is obtained, which is used in the next MD simulation. This iterative process is repeated until the electron distribution of the solute and the solvent structure around it become mutually equilibrated. Details of the method can be found elsewhere.<sup>25</sup>

Once the in-solution energy has been calculated for the ground and excited states, the solvent shift can be obtained as the difference:

$$\begin{aligned} \delta &= \Delta E - \Delta E^0 \\ &= (\langle \Psi_{\text{ex}} | \hat{H}_{\text{QM}} + \hat{V} | \Psi_{\text{ex}} \rangle - \langle \Psi_{\text{g}} | \hat{H}_{\text{QM}} + \hat{V} | \Psi_{\text{g}} \rangle) \\ &\quad - (\langle \Psi_{\text{ex}}^0 | \hat{H}_{\text{QM}}^0 | \Psi_{\text{ex}}^0 \rangle - \langle \Psi_{\text{g}}^0 | \hat{H}_{\text{QM}}^0 | \Psi_{\text{g}}^0 \rangle) \end{aligned} \quad (1)$$

where the subscripts ex and g denote the excited and ground state of the transition,  $H_{\text{QM}}$  is the QM Hamiltonian of the solute at the in-solution geometry, without the solute–solvent interaction,  $\hat{V}$ , and  $\hat{H}_{\text{QM}}^0$  is the QM Hamiltonian at the gas phase geometry;  $\Psi$  and  $\Psi^0$  are the wave functions optimized in solution and in the gas phase, respectively.

In a previous study by Martín et al.,<sup>25d</sup> the role of the solvent Stark effect on the electronic transitions for different chromophores in solution was analyzed. The solvent Stark values provide a measure of the errors introduced by the mean field approximation. It was found that the contribution of the solvent Stark effect is lower than 0.1 kcal/mol even in polar systems. These results validate the use of this approximation.

Some calculations were done taking into account the solvent polarization, that is, the response of the solvent electronic polarization to the changes in the solute charge distribution originated by the electron transition. To this end, once the equilibrium solvent structure was obtained with a non-polarizable solvent, a molecular polarizability was assigned to every solvent molecule, and simultaneously the effective solvent charge distribution used in the MD calculation was replaced by its gas-phase value. The dipole moment induced on each solvent molecule is a function of the dipole moments induced on the rest of the molecules and of the solute charge distribution, and hence the electrostatic equation has to be solved self-consistently. The process finishes when convergence in the solute and solvent charge distribution is achieved. For more details, we refer to previous works.<sup>26</sup>

**2.1. Computational Details.** All the in solution geometry optimizations were performed with the ASEP/MD program,<sup>23</sup> using the data provided by Gaussian 09<sup>27</sup> and Moldy.<sup>28</sup> The ground-state structure was described using the MP2 level of

theory. In order to study the absorption spectra, electronic states were described using SA-CASSCF. A systematic study for every solvent was done employing a different number of roots for state averaging. From the analysis of the data, it results that the best description of the absorption transition is obtained with three roots for cHex and MeOH and five roots for DCM. All the roots had equal weights. All electrons of the  $\pi$  skeleton were included in the active space, that is, 10  $\pi$  electrons in 10 orbitals (10e, 10o) for the five-double-bond models M1 and M2 and 12 valence  $\pi$  electrons in 12 orbitals (12e, 12o) for the complete chromophore with six double bonds, PSB11. Dynamic electron correlation was included by using a second order perturbation method, CASPT2. For all the multi-configurational calculations we employed the MOLCAS 7.4 program.<sup>29</sup> The split-valence 6-31G(d) basis set was used in order to facilitate comparison with previous studies. We did all the calculations with no IPEA (ionization potential-electron affinity) shift to be consistent with previous calculations done with older MOLCAS versions.<sup>30</sup> An additional imaginary shift of 0.1i  $E_h$  was included in order to minimize the appearance of intruder states.

The number of molecules that were included in the simulations was determined by the size of the solvent molecule in order to reach a compromise between the box size (35 Å for MeOH and DCM and 40 Å for cHex) and the computational cost. In this way, we included 630 molecules for methanol and 350 for both cHex and DCM. All molecules were simulated at fixed intramolecular geometry by combining Lennard-Jones interatomic interactions with electrostatic interactions. The solvent and solute molecules were represented using AMBER nonbonded parameters.<sup>31</sup> For the chloride counterion, also AMBER-99 force field parameters of monovalent ions were employed.<sup>32</sup> Periodic boundary conditions were applied, and spherical cutoffs were used to truncate the molecular interactions at 9.0 Å. A time step of 0.5 fs was used. The electrostatic interaction was calculated with the Ewald method. The temperature was fixed at 298 K by using a Nosé-Hoover thermostat. Each MD simulation was run at constant volume for 75 ps (25 ps equilibration, 50 ps production). The total number of ASEP/MD cycles was 10, and the ASEP at each cycle was calculated from the data of 500 configurations evenly distributed along the simulation. In solution, final results were obtained by averaging the last five ASEP/MD cycles, and therefore they represent an effective simulation time of 250 ps.

### 3. RESULTS AND DISCUSSION

Previous to the analysis of the absorption spectra in solvents of different polarities, we analyzed the performance of some of the molecules commonly used as simplified models of the PSB11 molecule both in the gas phase and in methanol. Then, once the calculation level and the model to be studied were chosen, the influence of other solvents of different polarity, dichloromethane and cyclohexane, was examined. Finally, the counterion effect on the absorption bands' positions was studied. We have chosen as a counterion the chloride anion. In studying the ionic pair chromophore-chloride anion, several possibilities were considered. First, the study of the solute-counterion ionic pair in the gas phase was done. We name these calculations Cl(QM). Then, we examined the solvent and counterion effects on the absorption spectra in three solvents: cyclohexane, dichloromethane, and methanol. Here, both the counterion and the solvent were described classically during the MM simulation. These calculations are named cHex-Cl(MM),

DCM-Cl(MM), and MeOH-Cl(MM), respectively. The electron transitions were computed with only the solute in the quantum part and including several thousands of external point charges that represent the average perturbation of the counterion and the solvent. Finally, in a different set of calculations, named cHex-Cl(QM), the anion was quantum-mechanically described, and an analysis of the charge transfer between the counterion and the chromophore inside the solvent was performed.

**3.1. Solvent Shifts in Methanol Using Different Structural Models.** The geometry of the ground state was optimized at both the CASSCF and MP2 levels and the transition energies were calculated at CASPT2 level. Table 1

**Table 1. PSB11 Optimized Bond Lengths and BLA Values in the Gas Phase and in Methanol Solution at the MP2 and CASSCF Levels, in Å**

	gas phase		MeOH	
	MP2	CASSCF	MP2	CASSCF
C <sub>5</sub> –C <sub>6</sub>	1.37	1.35	1.36	1.35
C <sub>6</sub> –C <sub>7</sub>	1.46	1.49	1.47	1.48
C <sub>7</sub> –C <sub>8</sub>	1.37	1.35	1.36	1.35
C <sub>8</sub> –C <sub>9</sub>	1.44	1.47	1.45	1.47
C <sub>9</sub> –C <sub>10</sub>	1.39	1.36	1.38	1.36
C <sub>10</sub> –C <sub>11</sub>	1.41	1.45	1.43	1.46
C <sub>11</sub> –C <sub>12</sub>	1.39	1.36	1.37	1.36
C <sub>12</sub> –C <sub>13</sub>	1.42	1.46	1.44	1.47
C <sub>13</sub> –C <sub>14</sub>	1.40	1.37	1.38	1.36
C <sub>14</sub> –C <sub>15</sub>	1.40	1.42	1.41	1.44
C <sub>15</sub> –N	1.33	1.29	1.31	1.28
BLA	0.21	0.50	0.35	0.54

displays the values of the single–double bond length alternation (BLA) in the gas phase and in methanol at different levels of calculation for PSB11. The data corroborate a well-known fact: the CASSCF method provides geometries that tend to overestimate the BLA with respect to geometries optimized with methods that include dynamic correlation.<sup>33</sup> So, CASSCF geometries provide BLA values (see Table 1) higher than MP2 structures, both in a vacuum (0.50 Å versus 0.21 Å) and in methanol (0.54 Å versus 0.35 Å). This fact has direct consequences on the absorption spectra. Table 2 displays the

**Table 2. Electronic Transition Energies to the S<sub>1</sub> State for PSB11 in the Gas Phase and in Methanol Calculated at the CASPT2 Level, with CASSCF and MP2 Geometries and Their Respective Solvent Shifts  $\delta$  (All Values Are in eV)**

	gas phase	MeOH	$\delta$
CASPT2//CASSCF	2.35	3.35	1.00
CASPT2//MP2	1.96	2.73	0.77
experimental <sup>9</sup>	2.00	2.77	0.77

transition energies calculated for the complete PSB11 chromophore at two different levels, both in the gas phase and in methanol. The last column provides the solvent shift for the S<sub>0</sub> → S<sub>1</sub> transition, from which originates the most intense band in the absorption spectra. The transition energies calculated using CASSCF-optimized geometries are larger both in a vacuum and in methanol with respect to the MP2 structures. In methanol, the solvent shift for the CASSCF geometry is 0.23 eV larger than the experimental data. On the

other hand, when the dynamic correlation contribution is included both on the calculation of the transition energy and in the geometry optimization (CASPT2//MP2 calculation), the results agree with the experiment both in the gas phase and in a methanol solution; differences lower than 0.05 eV are found. Consequently, in the following sections we will employ the MP2 structures.

With respect to the performance of the different structural models, both reproduce the main characteristic of the experiment: two bands well separated in the gas phase,<sup>4</sup> assigned to transitions from the ground (covalent) state to the hole-pair (ionic) and the dot-dot (covalent) excited states, but only one broad band in methanol. In Table 3, the electron

**Table 3. Electronic Transition Energies from the Ground State to the Ionic and Covalent Excited States in a Vacuum and in Methanol Solution, and Solvent Shift Values for the Ionic Transition Calculated at the CASPT2 Level<sup>a</sup>**

	$S_0 \rightarrow$ ionic			$S_0 \rightarrow$ covalent	
	gas phase	MeOH	$\delta$	gas phase	MeOH
M1	2.59	3.63	1.04	3.45	3.90
M2	2.56	3.25	0.69	3.39	3.34
PSB11	1.96	2.73	0.77	2.88	3.24
exptl. <sup>9</sup>	2.00	2.77	0.77	3.22	

<sup>a</sup>All values are in eV.

transitions for the first two excited states and the solvent shift for the different models are shown. According to the experimental results, the solvent shift between methanol and the gas phase for the all-*trans* PSB11 chromophore is 0.77 eV.<sup>9</sup> As we have already indicated, the ASEP/MD method reproduces adequately the main characteristics of the PSB11 spectra in methanol. It is worth noting that the presence of the methyl groups, compare M1 and M2 results, does not affect the transition energy in a vacuum, but it modifies the solvent shift. So, the M1 model with no methyl groups yields two bands in the gas phase but only one broad band in solution, in agreement with the experiment; however, it overestimates the solvent shift by more than 0.4 eV. Figure 2 shows the radial distribution functions (rdf) between the solute nitrogen atom and the oxygen of the methanol molecules for the three models considered. The height of the first peak is similar in M2 and PSB11, and both are lower than the M1 value. It is clear that without methyl groups in the iminium end the solute–solvent

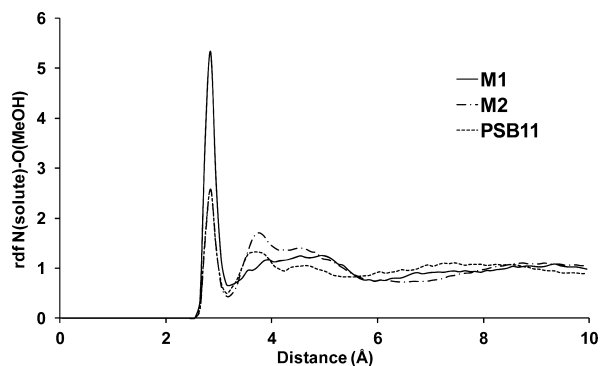


**Figure 2.** Radial distribution function  $N(\text{solute})\text{--O}(\text{MeOH})$  for the M1 and M2 models and the PSB11 chromophore.

interaction increases, and this is also reflected on the electronic transition values.

Regarding the electronic transition to the  $S_2$  state, considering that the oscillator strength for the covalent state is 1 order of magnitude lower than for the ionic one and that the experimental bandwidth of the absorption band in solution is around 0.6 eV, it is not possible to assign a precise value for this band in the experimental absorption spectrum. Our results show that the  $S_1\text{--}S_2$  energy differences, 0.1–0.5 eV depending on the model, are compatible with the observed bandwidth.

In sum, the presence of a methyl group attached to the nitrogen has no appreciable effect on the transition energies in the gas phase; however, it is crucial to adequately describe the solvation of these molecules because it modifies the ability of the iminium group to form hydrogen bonds with solvent molecules. Considering all these facts, the M2 model was employed in the rest of this study, as it combines a good description of the solvent shift with a reduced size that facilitates the computations.

**3.2. Solvent Shifts in Cyclohexane and Dichloromethane.** As it has already been indicated, the ASEP/MD method provides gas phase–methanol solvent shifts for PSB11 that agree with the experiment. However, the M2 model underestimates, with respect to PSB11, both the solvent shift of the first electron absorption band in 0.08 eV and the energy difference between the first and second excited states (in the gas phase) in about 0.4 eV. It is important to keep in mind these values when we analyze the performance of the M2 model in other solvents.

The computed electronic transition energies and the calculated and experimental solvent shift values are collected in Table 4. It is well-known that cHex acts as an inert solvent

**Table 4. Electronic Transition Energies to the Ionic and Covalent Excited States, Energy Differences between the Two Excited States,  $\Delta_{\text{Ionic-Coval}}$ , Calculated Solvent Shift to the Ionic Excited State  $\delta$ , and Their Corresponding Experimental Values<sup>a</sup>**

	$S_0 \rightarrow$ ionic	$\delta$	$\delta$ exp <sup>9</sup>	$S_0 \rightarrow$ coval.	$\Delta_{\text{Ionic-Coval}}$
gas phase	2.56			3.39	0.83
Cl (QM)	3.56	1.00		3.65	0.09
cHex	2.58	0.02	0.63	3.36	0.78
cHex-Cl(MM)	3.29	0.73		3.43	0.14
cHex-Cl(QM)	3.31	0.75		3.46	0.15
DCM	3.07	0.51	0.61	3.11	0.04
DCM-Cl(MM)	3.09	0.53		3.48	0.39
MeOH	3.25	0.69	0.77	3.34	0.09

<sup>a</sup>All values are in eV. Calculated values refer to the M2 model; experimental values are for PSB11.

that causes a poor solvation, and therefore, it should induce a negligible solvent shift. Indeed, there are no changes in the solute structural parameters with respect to the gas phase geometry. Consequently, the calculated absorption spectrum in cHex should be very similar to the gas-phase one with an absorption transition energy close to 2.56 eV. However, the experimental absorption spectrum of PSB11 in a nonpolar solvent as is cHex shows a solvent shift of 0.63 eV.<sup>9</sup> This large solvent shift cannot be explained by the solvent polarity of cyclohexane. In fact, the value that ASEP/MD provides for this solvent is very close to that obtained in the gas phase.

Consequently, we must search for another cause for the large solvent shift in cHex.

When we pass to the DCM solvent, our calculations provide a solvent shift of 0.51 eV, somewhat lower than the experimental value of 0.61 eV. However, the DCM–MeOH experimental shift of 0.16 eV is very well reproduced. So, the discrepancy is attributable to the use of a simplified model. We note that no significant differences were found in the solute geometry in the different solvents (see Table S.1 in the Supporting Information). Thus, the structural parameters are similar to those shown for the MP2/MeOH case in Table 1. In addition, gas-phase calculations done with in-solution optimized geometries showed that the slight geometry differences do not have a significant influence on the electron transition energies. A study of Röhrig et al.<sup>34</sup> showed that this chromophore displays a great flexibility in solution when it is simulated by both classical and Car–Parrinello molecular dynamics. However, these dynamic fluctuations have effects in the increase of the bandwidth and not in the prediction of the maximum of the band, which is what we calculate with our method.

**3.3. Simultaneous Counterion and Solvent Effects on the Transition Energy.** As previously indicated, the experimental solvent shifts found in nonpolar solvents are similar to those of polar solvents, with differences of only 0.1 eV between them, and absolute values close to 0.6–0.8 eV. As we have shown above, the large value in cHex cannot be explained by the solvent polarity, and other mechanisms must be proposed.

In order to ensure protonation of the chromophore, the experimental absorption measurements are usually performed with samples prepared with an excess of a strong acid like trifluoroacetic or trichloroacetic. It has been proposed<sup>9</sup> that the large hypsochromic shift found with less polar solvents such as cHex compared to polar solvent results is due to two main reasons: intramolecular interactions and homoconjugation of the counterion.<sup>35</sup> We propose that it is the presence of the counterion which plays the main role in the solvation process for nonpolar solvents.

A previous computational study by Cembran et al.<sup>5</sup> pointed to the significant effect of the counterion on the potential energy surfaces of a retinal model in the gas phase. Indeed, employing chloride as a counterion and at the ground state minimum geometry, the first two excited states were quasi-degenerate, whereas in the absence of the ion the states were well separated. This effect is similar to that produced by polar solvents. On the other hand, Tomasello et al.<sup>16</sup> simulated with molecular dynamics the closest amino acids to the chromophore in the rhodopsin protein and analyzed their effect in the absorption spectrum. They concluded that the major effect in the electronic transitions comes from the closest charged counterion Glu-113, which produces a significant blue shift of the charge-transfer band.

In order to check the validity of our hypothesis, we repeated our study of the solvent shift but including now the counterion effect. We began by checking that in polar solvents like methanol, the counterion is well solvated and therefore does not directly interact with the chromophore. In fact, if we start the simulation with the counterion forming an ionic pair with the solute, in the calculation named MeOH–Cl(MM), in a short time the two ions become completely separated, and the transition energies are those obtained without the counterion in the same solvent. So, the shift in the transition energies in

methanol can be fully assigned to the solvent effect. These results agree with the ones obtained in previous studies by Rajamani and Gao<sup>36</sup> and Röhrig et al.<sup>34</sup> using also chloride as a counterion. These authors found that because of the large dielectric screening effect of methanol, the effect of the counterion on the structure and spectrum of the solute is minimal. This has been corroborated by experiments showing that the position of the chromophore absorption band in polar solvents is not affected by the nature of the counterion.<sup>37</sup>

On the contrary, in cHex the counterion is poorly solvated, and it remains close to the solute forming an ionic pair. In our study, the chloride counterion was treated in different ways. In a first calculation, named Cl(QM), the ionic pair was studied in the gas phase. In a second set of calculations, named cHex–Cl(MM), DCM–Cl(MM), and MeOH–Cl(MM), the counterion was treated together with the solvent classically; that is, the quantum mechanical subsystem includes only the solute, whereas the counterion together with the solvent molecules is included only through a molecular mechanics force field during the MD simulations and represented as averaged point charges in the quantum calculations. In a final calculation, named cHex–Cl(QM), both the solute and the chloride anion were included as part of the QM subsystem in the calculation in solution. In all cases, quantum or classical treatment, gas phase or in solution conditions (except in the MeOH–Cl(MM) calculation, as reported above), the counterion remained close to the acidic hydrogen (see Figure 3). Our goal in the following

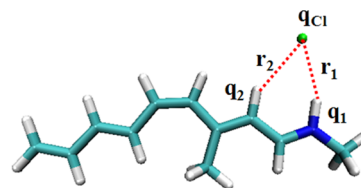


**Figure 3.** Representation of the main hydrogen-bond lengths and atomic charges for the atoms implied in the hydrogen bonds in the counterion–M2 structure.

sections is trying to answer the following questions: (1) How does the presence of the counterion affect the rhodopsin chromophore? (2) Which is the influence of the possible counterion–solute charge transfer on the transition energies?

*a. Ionic Pair in the Gas Phase.* We begin by studying the M2–chloride ionic pair in the gas phase. We named this calculation Cl(QM). From a geometrical point of view, there are no significant changes in the solute structure with respect to the gas-phase geometry; only the acidic H–N distance is enlarged around 11% due to the strong M2–Cl interaction. The acidic H–counterion distance is 1.75 Å, and the N–H–Cl angle is linear with a value of 180°. These values are typical of a strong hydrogen bond as corresponds to charged molecules. The counterion–M2 closeness has direct consequences on the transition energy value, which takes now a value of 3.56 eV. Thus, the band shift originated by the counterion is (see Table 4) about 1.0 eV. Furthermore, and as a consequence of the proximity between the two ions, there is a large charge transfer between them. The chromophore electronic distribution represented as Mulliken charges is gathered in Table 5 for both the ground and ionic excited states. The charge distribution was split into three fragments: the counterion (Cl), the iminium part (C<sub>10</sub>–N), which includes the adjacent carbon and the bonded hydrogens, and the rest of the molecule

**Table 5. Mulliken Charges (in  $e$ ) for the Ground and Ionic Excited States in the Gas Phase and in the Cl(QM) Calculation**

	gas phase		Cl(QM)	
	$S_0$	ionic	$S_0$	ionic
$C_1-C_9$	+0.30	+0.62	+0.14	+0.40
$C_{10}-N$	+0.70	+0.38	+0.57	+0.31
Cl			-0.71	-0.71

( $C_1-C_9$ ). It can be observed that part of the chloride charge,  $0.29e$ , is transferred to the M2 molecule. In the ground state, this charge is evenly distributed between the two parts of the chromophore; consequently, as for the isolated chromophore, the remaining charge is mainly concentrated on the iminium part. The chloride anion, which is close to the positive part of the molecule, stabilizes to a greater extent the covalent ground state than the ionic excited state, where the positive charge is spread out over the entire molecule. Hence, the transition energy increases with respect to the gas-phase value. In order to understand the role played by the charge transfer, we recalculate the transition energy but replace the chloride atom with a point charge placed in the same position. In this case, the transition energy decreases to 3.26 eV. Clearly, the effect of the charge transfer between the chloride and the chromophore is to increase the transition energy.

*b. Ionic Pair in Cyclohexane.* Next, we go on to discuss the in solution results of the ionic pair. In a first set of calculations, the counterion was classically described together with the solvent; the calculation in cyclohexane is named cHex-Cl(MM). Table 6 displays the average Cl-H distances during

**Table 6. Cl-H Distances (in Å) and Atomic CHELPG<sup>38</sup> Charges for the Ground State (in  $e$ ) for the Counterion-M2 Structure (see Figure 3)**

	$r_1$	$r_2$	$q_1$	$q_2$	$q_{Cl}$
cHex-Cl(MM)	2.20	2.78	+0.47	+0.31	-1.00
DCM-Cl(MM)	2.32	3.08	+0.44	+0.27	-1.00

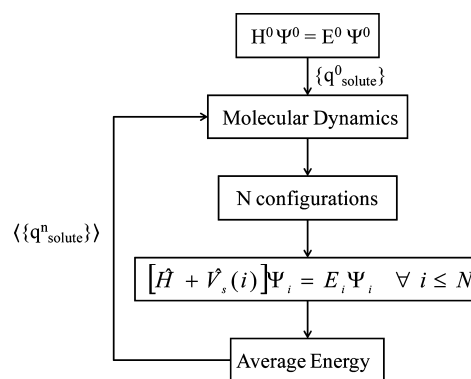
the molecular dynamics simulation and the ground-state charges for the involved atoms (see Figure 3). We can observe the increase of the Cl-H distance to 2.20 Å with respect to the distance obtained in the gas phase. Furthermore, whereas the Cl(QM) structure shows a perfect linear N-H-Cl angle, in solution the angle is 170°. Now the closest *syn*-hydrogen, due to its large positive charge, plays a non-negligible role interacting with the counterion.

The cHex-Cl(MM) results provide a solvent shift of 0.73 eV (see Table 4), a value that slightly overestimates the experimental solvent shift of 0.63 eV. It is clear that the presence of the counterion originates a much larger solvent shift than in the calculation without the counterion. However, with respect to the Cl(QM) calculation, this solvent shift is significantly lower, which is an improvement toward the experimental shift in cyclohexane. There are in principle three main factors that can account for this difference: the lack of charge transfer between counterion and solute in cHex-Cl(MM), the different position of the counterion, and the reaction field originated by the cyclohexane molecules. The effect of the cyclohexane molecules reaction field is expected to be minimal, as corresponds to a nonpolar solvent, and is confirmed in the cHex calculation without a counterion.

Moreover, when the solvent electron polarization is included in the calculations, the solvent shift is only slightly affected, decreasing to 0.70 eV. The other two factors work in the same direction: the lack of charge transfer and the increase in the Cl-H distance both decrease the transition energy and explain the lower value in cHex-Cl(MM) with respect to Cl(QM).

In conclusion, one of the main reasons behind the improvement with respect to the ionic pair in the gas phase can be found in the aforementioned change in the chloride position with respect to the M2 molecule. In fact, one of the causes why gas-phase calculations are not a valid model for the ionic pair in solution is that they do not take into account the effect that thermal agitation has on the cation-anion distance. Regarding the small discrepancy between our results and the experimental data, we give a reminder that the latter refer to the complete PSB11 chromophore while the former are for the M2 model, and additionally the counterion is different in the two cases: trifluoroacetate (a bidentate anion) in the experiments and chloride (a monodentate anion) in our calculations.

One criticism that can be made of our in-solution calculations is that they do not account for a possible counterion-solute charge transfer since during the molecular dynamics calculation the chloride is described as a point charge. The charge transfer between the two ions can be accounted for if the chloride anion is included in the quantum part of the system. In order to analyze the contribution of this fact (see cHex-Cl(QM) result in Table 4), we use a modification of the ASEP/MD method. The basic scheme is displayed in Figure 4.

**Figure 4. QM/MD scheme for the cHex-Cl(QM) calculation.**

In these calculations, the chloride was classically simulated together with the cHex, and then, 50 configurations were extracted. Next, 50 QM calculations were performed for each solvent configuration where the counterion was included in the quantum calculation, and the cHex solvent molecules were represented as point charges. From these 50 QM calculations, we can evaluate the average counterion-solute charge transfer, by averaging the CHELPG charges for both solute and counterion. Finally, these average charges that include the charge transfer effect are introduced in a new molecular dynamics simulation. This process is repeated as usual for several cycles until convergence. Electronic transition energies were calculated for the 50 configurations of the last cycle. It is worth noting that in these calculations the solute geometry was not reoptimized, as it was found in test calculations that further optimizing the geometry in this case hardly has any effect.

That said, some interesting conclusions can be extracted from the charge-transfer test. First, a counterion→solute charge

transfer of  $0.14e$  took place, smaller than the value found in the gas phase. This lower charge transfer in solution is probably due to the larger cation–anion distance. The  $0.14e$  transferred to the M2 is distributed mainly in the iminium part of the molecule, especially in the acidic-H,  $-0.18e$ , and in the nitrogen  $+0.15e$  (see Figure 3). The effect of the quantum-mechanical description of the chloride atom on the total solvent shift is small. The increase in the solvent shift value, calculated as an average of 50 configurations, was  $0.02$  eV. This low value is the result of two opposite effects. On the one hand, the average Cl–solute distance increases with respect to the cHex-Cl(MM) case, and according to this the transition energy should decrease. On the other hand, the charge transferred from the counterion to the solute is localized in the iminium part of the molecule (see Table 7). This new charge distribution stabilizes

**Table 7. Atomic CHELPG Charges (in  $e$ ) for the Ground State of M2 for the cHex-Cl(MM) and cHex-Cl(QM) Calculations**

	cHex-Cl(MM)	cHex-Cl(QM)
C <sub>1</sub> –C <sub>9</sub>	+0.14	+0.14
C <sub>10</sub> –N	+0.86	+0.72
Cl	–1.00	–0.86

the covalent ground state with respect to the case without charge transfer, and hence the electronic transition energy increases. The sum of these two effects yields an almost negligible increase of the solvent shift value.

*c. Ionic Pair in Dichloromethane.* Although the experimental solvent shift in dichloromethane is well reproduced with the influence of the dichloromethane molecules alone (see Table 4 above, DCM calculation), we followed the same process as in cHex, and we included the chloride counterion in the molecular simulations. Unlike in the MeOH-Cl(MM) calculation, the lower polarity of the DCM molecules permits the chloride to remain close to the chromophore, forming an ionic pair. However, it is striking that the solvent shift obtained when the chloride anion is included into the molecular dynamics simulation barely changes, with a value of  $0.53$  eV. The average N–Cl length is slightly larger, about  $0.12$  Å, than in the cHex-Cl(MM) case. The DCM molecules solvate better the chloride than the cHex and cause a slight increase of the counterion–solute distance. The decrease in the ground-state atomic charges on the chromophore acidic-H and its *syn*-H atoms ( $q_1$  and  $q_2$ , see Table 6) is in accord with the increase of the H–Cl distances.

Given that, in principle, the solvent shift increases with increasing solvent polarity, it seems counterintuitive that the shift in the DCM-Cl(MM) calculation is lower than in the cHex-Cl(MM) one. In order to explain this fact, we analyze more in depth the origin of the solvent shift in DCM-Cl(MM). There are two main contributions to the solvent shift: the counterion effect and the orientational polarization of the DCM molecules. When only the effect of the counterion (obtained from 500 configurations of the solute+anion molecular dynamics) is considered, the solvent shift increases to  $0.70$  eV, which is very similar to the cHex-Cl(MM) result. It then appears that the DCM molecules exert an opposite effect on the solvent shift depending on the presence or not of the counterion ( $+0.50$  eV in the DCM calculation,  $-0.17$  eV in the DCM-Cl(MM) one). This can be explained as a consequence of the reorientation of the solvent molecules around the

chloride–solute ion pair: the reaction field changes with respect to the case of neat DCM. This can be illustrated with the rdf's between the acidic hydrogen of M2 and the Cl and H atoms of the dichloromethane molecules, shown in Figure 5. In the case

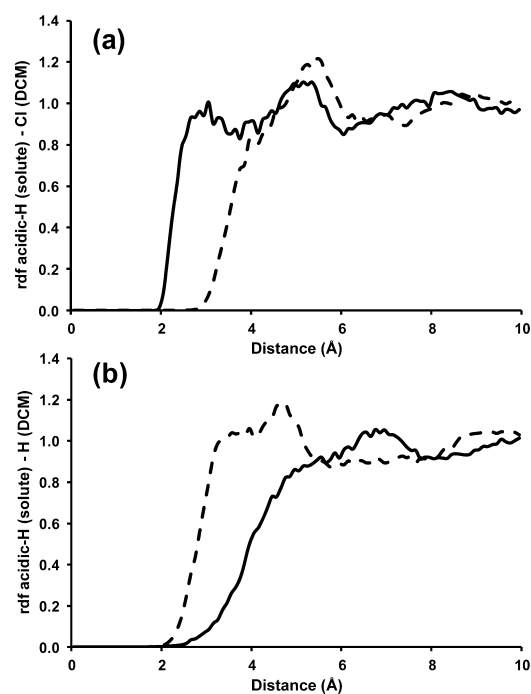


**Figure 5.** Radial distribution function for (a) acidic-H(M2)-Cl(DCM) and (b) acidic-H(M2)-H(DCM) for the DCM calculation (full line) and DCM-Cl(MM) (dotted line).

of the DCM solvent without a counterion, the DCM molecules are oriented with the chloride atoms pointing to the part with a lower electron density, that is, the iminium part. In the DCM-Cl(MM) case, however, the anion changes the orientation of the DCM molecules. Thus, the solvent molecules around the ion pair flip over, pointing the hydrogens toward the counterion. These two effects, together with the influence of the counterion, determine that the final solvent shift obtained in DCM with and without a counterion is almost the same.

**3.3. Solvent and Counterion Effects on the Ionic and Covalent Excited State Energy Differences.** An important aspect to consider, because of its possible effect on the photoisomerization mechanism, is the relative position of the first and second excited states. In the gas phase, the two excited states, ionic and covalent, are separated by about  $0.8$ – $1.0$  eV depending on the model considered. However, when the molecule is in the presence of a counterion or a polar solvent, the two states become almost degenerate, see Table 4. Most energy differences are comprised between  $0.09$  and  $0.16$  eV. The most striking value corresponds to the DCM-Cl(MM) calculation, where the energy difference increases to  $0.39$  eV. Note that the presence of the counterion+DCM has roughly the same effect that the neat solvent does on the position of the ionic state; however the effect on the covalent excited state is different. In the DCM-Cl(MM) calculation, we can split the Cl and solvent contributions, so the effect of the Cl anion is to decrease the covalent–ionic excited state difference down to  $0.09$  eV, in agreement with the rest of the values. On the contrary, the effect of the DCM molecules is to increase the energy difference up to  $0.39$  eV; we should provide a reminder

that in the presence of the counterion the DCM molecules orient themselves in a completely different way around the chromophore. This result is interesting because it mimics the expected behavior inside the protein, where we have a polarizable surrounding around an ionic pair formed by the protein and the Glu-113 residue. In any case, given the different behavior of the M2 model and the complete chromophore, these results must be taken with caution.

#### 4. CONCLUSIONS

A complete analysis of the solvent and counterion effects on the absorption spectra of a valid model of the PSB11 chromophore has been carried out. Our model, M2, reproduces the main characteristics of the complete chromophore, including the presence of one acidic hydrogen in the iminium part, which confers solvation properties similar to those of PSB11. Solvents of different polarities have been analyzed, such as the nonpolar cyclohexane, the slightly polar solvent dichloromethane, and the polar and protic solvent methanol. Furthermore, the presence of explicit counterions, quantum-mechanically and classically described, has been considered.

The first conclusion is that the structural parameters of the solute are hardly altered in all solvents employed, and therefore the effect of the intramolecular geometry change on the solvent shift values is practically negligible. Regarding the solvent polarity, we have found three different cases. First, we show that to explain the large solvent shifts found for apolar solvents, it is compulsory to include the counterion effect. However, the ionic pair in the gas phase is not a good model as the solvent shift is clearly overestimated in this way. When the thermal agitation due to the solvent is considered, then the N–Cl distance increases. Due to this, the solvent shift decreases with respect to the gas-phase ionic-pair result. Second, the solvent shift caused by DCM is independent of the counterion presence. When the chloride is included, two opposite effects occur: on the one hand, the Cl–M2 interaction increases the solvent shift as in the cHex-Cl(MM) case; on the other hand, the molecular reorganization around the ion pair partially cancels the previous effect. The final result leads to a solvent shift value in agreement with the calculation without a counterion and the experiments. Third, the polarity of the methanol causes a good solvation of the counterion that prevents the formation of the solute and chloride ionic pair; in this case, the transition energy shift is fully explained only by solvation effects of the methanol molecules.

A new methodology, which is derivative from ASEP/MD, was tested. This method permits one to consider the charge transfer between the anion and the solute. The results of cHex-Cl(QM) calculations barely change the solvent shift, with an increase of 0.02 eV in its value. In this case, the increase in the solvent shift due to the counterion is canceled by the extra ground-state electron density, which makes the iminium part less positive. Consequently, the ground state loses its covalent nature (shows a lower charge separation) and is destabilized, decreasing the solvent shift.

#### ■ ASSOCIATED CONTENT

##### ■ Supporting Information

ASEP/MD scheme and M2 optimized bond lengths. This material is available free of charge via the Internet at <http://pubs.acs.org>.

#### ■ AUTHOR INFORMATION

##### Corresponding Author

\*E-mail: [auroram1@unex.es](mailto:auroram1@unex.es).

##### Notes

The authors declare no competing financial interest.

#### ■ ACKNOWLEDGMENTS

This work was supported by the CTQ2008-06224/BQU Project from the Ministerio de Ciencia e Innovación of Spain, cofinanced by the European Regional Development Fund (ERDF), and the PRI08A056 Project from the Consejería de Economía, Comercio e Innovación of the Gobierno de Extremadura. I.F.G. acknowledges the Gobierno de Extremadura and the European Social Fund for financial support. A.M.-L. acknowledges financial support from the Juan de la Cierva subprogramme of the Ministerio de Economía y Competitividad of Spain. The authors also thank the Fundación Computación y Tecnologías Avanzadas de Extremadura (COMPUTAEX) for additional computational resources.

#### ■ REFERENCES

- (1) Schoenlein, W. P.; Peteanu, L. A.; Mathies, R. A.; Shank, C. V. *Science* **1991**, *254*, 412.
- (2) Wang, Q.; Schoenlein, R. W.; Peteanu, L. A.; Mathies, R. A.; Shank, C. A. *Science* **1994**, *266*, 422.
- (3) Kandori, H.; Katsuta, Y.; Ito, M.; Sasabe, H. *J. Am. Chem. Soc.* **1995**, *117*, 2669.
- (4) Nielsen, I. B.; Lammich, L.; Andersen, L. H. *Phys. Rev. Lett.* **2006**, *96*, 018304.
- (5) Cembran, A.; González-Luque, R.; Altoè, P.; Merchán, M.; Bernardi, F.; Olivucci, M.; Garavelli, M. *J. Phys. Chem. A* **2005**, *109*, 6597.
- (6) Hurlley, J. B.; Ebrey, T. G.; Honig, B.; Ottolenghi, M. *Nature* **1977**, *270*, 540.
- (7) Schapiro, I.; Ryazantsev, M. N.; Manuel Frutos, L.; Ferré, N.; Lindh, R.; Olivucci, M. *J. Am. Chem. Soc.* **2011**, *133*, 3354.
- (8) Altun, A.; Yokoyama, S.; Morokuma, K. *J. Phys. Chem. B* **2008**, *112*, 16883.
- (9) Zgrablić, G.; Haacke, S.; Chergui, M. *J. Phys. Chem. B* **2009**, *113*, 4384.
- (10) Freedman, K. A.; Becker, R. S. *J. Am. Chem. Soc.* **1986**, *108*, 1245.
- (11) Muñoz-Losa, A.; Fdez. Galván, I.; Aguilar, M. A.; Martín, M. E. *J. Phys. Chem. B* **2008**, *112*, 8815.
- (12) Muñoz-Losa, A.; Fdez. Galván, I.; Martín, M. E.; Aguilar, M. A. *J. Phys. Chem. B* **2006**, *110*, 18064.
- (13) Warshel, A. *J. Chem. Phys.* **1979**, *83*, 1640.
- (14) Toniolo, A.; Ben-Nun, M.; Martínez, T. J. *J. Phys. Chem. A* **2002**, *106*, 4679.
- (15) Burghardt, I.; Cederbaum, L.; Hynes, J. T. *Faraday Discuss.* **2004**, *127*, 395.
- (16) Tomasello, G.; Olaso-González, G.; Altoè, P.; Stenta, M.; Serrano-Andrés, L.; Merchán, M.; Orlandi, G.; Bottoni, A.; Garavelli, M. *J. Am. Chem. Soc.* **2009**, *131*, 5172.
- (17) Mori, T.; Nakano, K.; Kato, S. *J. Chem. Phys.* **2010**, *133*, 064107.
- (18) Ruckebauer, M.; Barbatti, M.; Mueller, T.; Lischka, H. *J. Phys. Chem. A* **2010**, *114*, 6757.
- (19) Li, X.; Chung, L. W.; Morokuma, K. *J. Chem. Theory Comput.* **2011**, *7*, 2694.
- (20) Rajamani, R.; Lin, Y.-L.; Gao, J. *J. Comput. Chem.* **2011**, *32*, 854.
- (21) Kaila, V. R. I.; Send, R.; Sundholm, D. *J. Phys. Chem. B* **2012**, *116*, 2249.
- (22) Gozem, S.; Schapiro, I.; Ferré, N.; Olivucci, M. *Science* **2012**, *337*, 122.
- (23) Fdez. Galván, I.; Sánchez, M. L.; Martín, M. E.; Olivares del Valle, F. J.; Aguilar, M. A. *Comput. Phys. Commun.* **2003**, *155*, 244.



(24) Cembran, A.; Bernardi, F.; Olivucci, M.; Garavelli, M. *Proc. Natl. Acad. Sci. U. S. A.* **2005**, *102*, 6255.

(25) (a) Sánchez, M. L.; Martín, M. E.; Aguilar, M. A.; Olivares del Valle, F. J. *J. Comput. Chem.* **2000**, *21*, 705. (b) Martín, M. E.; Sánchez, M. L.; Olivares del Valle, F. J.; Aguilar, M. A. *J. Chem. Phys.* **2002**, *116*, 1613. (c) Sánchez, M. L.; Martín, M. E.; Fdez. Galván, I.; Olivares del Valle, F. J.; Aguilar, M. A. *J. Phys. Chem. B* **2002**, *106*, 4813. (d) Martín, M. E.; Sánchez, M. L.; Corchado, J. C.; Muñoz-Losa, A.; Fdez. Galván, I.; Olivares del Valle, F. J.; Aguilar, M. A. *Theor. Chem. Acc.* **2011**, *128*, 783.

(26) Martín, M. E.; Muñoz-Losa, A.; Fdez.-Galván, I.; Aguilar, M. A. *J. Chem. Phys.* **2004**, *121*, 3710.

(27) Frisch, M. J.; Trucks, G. W.; Schlegel, H. B.; Scuseria, G. E.; Robb, M. A.; Cheeseman, J. R.; Scalmani, G.; Barone, V.; Mennucci, B.; Petersson, G. A.; Nakatsuji, H.; Caricato, M.; Li, X.; Hratchian, H. P.; Izmaylov, A. F.; Bloino, J.; Zheng, G.; Sonnenberg, J. L.; Hada, M.; Ehara, M.; Toyota, K.; Fukuda, R.; Hasegawa, J.; Ishida, M.; Nakajima, T.; Honda, Y.; Kitao, O.; Nakai, H.; Vreven, T.; Montgomery, J. A., Jr.; Peralta, J. E.; Ogliaro, F.; Bearpark, M.; Heyd, J. J.; Brothers, E.; Kudin, K. N.; Staroverov, V. N.; Kobayashi, R.; Normand, J.; Raghavachari, K.; Rendell, A.; Burant, J. C.; Iyengar, S. S.; Tomasi, J.; Cossi, M.; Rega, N.; Millam, N. J.; Klene, M.; Knox, J. E.; Cross, J. B.; Bakken, V.; Adamo, C.; Jaramillo, J.; Gomperts, R.; Stratmann, R. E.; Yazyev, O.; Austin, A. J.; Cammi, R.; Pomelli, C.; Ochterski, J. W.; Martin, R. L.; Morokuma, K.; Zakrzewski, V. G.; Voth, G. A.; Salvador, P.; Dannenberg, J. J.; Dapprich, S.; Daniels, A. D.; Farkas, Ö.; Foresman, J. B.; Ortiz, J. V.; Cioslowski, J.; Fox, D. J. *Gaussian 09*, revision A.1; Gaussian, Inc.: Wallingford, CT, 2009.

(28) Refson, K. *Comput. Phys. Commun.* **2000**, *126*, 310.

(29) Aquilante, F.; De Vico, L.; Ferré, N.; Ghigo, G.; Malmqvist, P.-Å.; Neogrády, P.; Pedersen, T. B.; Pitoňák, M.; Reiher, M.; Roos, B. O.; Serrano-Andrés, L.; Urban, M.; Veryazov, V.; Lindh, R. *J. Comput. Chem.* **2010**, *31*, 224.

(30) Ghigo, G.; Roos, B. O.; Malmqvist, P.-Å. *Chem. Phys. Lett.* **2004**, *396*, 142.

(31) Cornell, W. D.; Cieplack, P.; Bayly, C. I.; Groud, K. M.; Ferguson, D. M.; Spellmeyer, D. C.; Fox, T.; Cladwell, J. W.; Kollman, P. A. *J. Am. Chem. Soc.* **1995**, *117*, 5179.

(32) Chen, A. A.; Pappu, R. V. *J. Phys. Chem. B Lett.* **2007**, *111*, 11884.

(33) Valsson, O.; Angeli, C.; Filippi, C. *Phys. Chem. Chem. Phys.* **2012**, *14*, 11015.

(34) Röhrig, U. F.; Guidoni, L.; Rothlisberger, U. *ChemPhysChem* **2005**, *6*, 1836.

(35) Baasov, T.; Sheves, M. *J. Am. Chem. Soc.* **1985**, *107*, 7524.

(36) (a) Rajamani, R.; Gao, J. *J. Comput. Chem.* **2002**, *23*, 96.

(b) Rajamani, R.; Gao, J. *J. Comput. Chem.* **2010**, *32*, 854.

(37) Platz, P. E.; Moheler, J. H. *Biochemistry* **1975**, *14*, 2340.

(38) (a) Chirlilan, L. E.; Francl, M. M. *J. Comput. Chem.* **1987**, *8*, 894.

(b) Breneman, C. M.; Wiberg, K. B. *J. Comput. Chem.* **1990**, *11*, 316.